



# The *FES* Gene at the 15q26 Coronary-Artery-Disease Locus Inhibits Atherosclerosis

Elisavet Karamanavi, David G. McVey<sup>1</sup>, Sander W. van der Laan<sup>1</sup>, Paulina J. Stanczyk, Gavin E. Morris, Yifan Wang<sup>1</sup>, Wei Yang, Kenneth Chan<sup>1</sup>, Robin N. Poston, Jun Luo, Xinmiao Zhou<sup>1</sup>, Peng Gong, Peter D. Jones, Junjun Cao, Renata B. Kostogrys<sup>1</sup>, Tom R. Webb<sup>1</sup>, Gerard Pasterkamp<sup>1</sup>, Haojie Yu<sup>1</sup>, Qingzhong Xiao<sup>1</sup>, Peter A. Greer, Emma J. Stringer, Nilesh J. Samani<sup>1</sup>, Shu Ye<sup>1</sup>

**BACKGROUND:** Genome-wide association studies have discovered a link between genetic variants on human chromosome 15q26.1 and increased coronary artery disease (CAD) susceptibility; however, the underlying pathobiological mechanism is unclear. This genetic locus contains the *FES* (FES proto-oncogene, tyrosine kinase) gene encoding a cytoplasmic protein-tyrosine kinase involved in the regulation of cell behavior. We investigated the effect of the 15q26.1 variants on *FES* expression and whether *FES* plays a role in atherosclerosis.

**METHODS AND RESULTS:** Analyses of isogenic monocytic cell lines generated by CRISPR (clustered regularly interspaced short palindromic repeats)-mediated genome editing showed that monocytes with an engineered 15q26.1 CAD risk genotype had reduced *FES* expression. Small-interfering-RNA-mediated knockdown of *FES* promoted migration of monocytes and vascular smooth muscle cells. A phosphoproteomics analysis showed that *FES* knockdown altered phosphorylation of a number of proteins known to regulate cell migration. Single-cell RNA-sequencing revealed that in human atherosclerotic plaques, cells that expressed *FES* were predominately monocytes/macrophages, although several other cell types including smooth muscle cells also expressed *FES*. There was an association between the 15q26.1 CAD risk genotype and greater numbers of monocytes/macrophage in human atherosclerotic plaques. An animal model study demonstrated that *Fes* knockout increased atherosclerotic plaque size and within-plaque content of monocytes/macrophages and smooth muscle cells, in apolipoprotein E-deficient mice fed a high fat diet.

**CONCLUSIONS:** We provide substantial evidence that the CAD risk variants at the 15q26.1 locus reduce *FES* expression in monocytes and that *FES* depletion results in larger atherosclerotic plaques with more monocytes/macrophages and smooth muscle cells. This study is the first demonstration that *FES* plays a protective role against atherosclerosis and suggests that enhancing *FES* activity could be a potentially novel therapeutic approach for CAD intervention.

**GRAPHIC ABSTRACT:** A graphic abstract is available for this article.

**Key Words:** atherosclerosis ■ coronary artery disease ■ *FES* ■ genetics ■ monocytes

Genome-wide association studies (GWAS) have discovered an association between single-nucleotide polymorphisms (SNPs) on chromosome 15q26.1 and increased coronary artery disease (CAD) susceptibility, in subjects consisting of mostly Europeans but also South Asians, East Asians, and Hispanic and African Americans.<sup>1–3</sup> However, the pathobiological mechanism

through which these genetic variants influence CAD risk is not fully understood.

rs17514846 has been reported as the lead CAD-associated SNP at the 15q26.1 locus in GWAS.<sup>1</sup> It is in high linkage disequilibrium (LD,  $r^2 \geq 0.8$ ) with several other SNPs in this genomic region. Due to strong LD, it is unclear from GWAS at the population level which SNP(s) at this

Correspondence to: Shu Ye, MD, PhD, Centre for Translational Medicine (MD6), National University of Singapore, 14 Medical Drive, Singapore 117599. Email shuye68@nus.edu.sg

Supplemental Material is available at <https://www.ahajournals.org/doi/suppl/10.1161/CIRCRESAHA.122.321146>

For Sources of Funding and Disclosures, see page 1016.

© 2022 The Authors. *Circulation Research* is published on behalf of the American Heart Association, Inc., by Wolters Kluwer Health, Inc. This is an open access article under the terms of the [Creative Commons Attribution Non-Commercial-NoDerivs](https://creativecommons.org/licenses/by-nc-nd/4.0/) License, which permits use, distribution, and reproduction in any medium, provided that the original work is properly cited, the use is noncommercial, and no modifications or adaptations are made.

*Circulation Research* is available at [www.ahajournals.org/journal/res](http://www.ahajournals.org/journal/res)

## Novelty and Significance

### What Is known?

- There is an association between genetic variants on chromosome 15q26.1 and increased coronary artery disease (CAD) susceptibility; however, the underlying biological mechanism is unclear.
- The gene encoding the FES (FES proto-oncogene, tyrosine kinase) protein kinase is located at the 15q26.1 locus; however, it is unknown if FES plays a role in atherosclerosis, the pathological condition underlying CAD.

### What New Information Does This Article Contribute?

- Our study shows that the CAD risk variants at the 15q26.1 locus reduce FES expression in monocytes.
- Experimentally attenuating the expression of FES in monocytes can increase monocyte migration.
- Knockout of FES in a mouse model increases atherosclerotic plaque sizes and in-plaque monocyte/macrophage abundance.

Recent studies have discovered a relationship between DNA variants on chromosome 15 and increased susceptibility to CAD, a common disease caused by atherosclerotic plaque development in arteries, but the molecular and cellular basis of this genetic association is unclear. Our present study shows that these DNA variants reduce the level of the protein kinase FES in monocytes and increase monocyte mobility, that there is a greater abundance of monocytes in atherosclerotic plaques of patients carrying the CAD risk-associated DNA variants, and that knockout of the orthologous gene of *FES* increases atherosclerotic plaque sizes and in-plaque monocyte abundance in an animal model. This study is the first demonstration that FES plays a protective role against atherosclerosis and provides a new insight into the biological mechanism underlying the association of the chromosome 15 genetic variants with CAD susceptibility. These findings suggest that enhancing FES activity could be a potentially novel therapeutic approach for the treatment of CAD.

## Nonstandard Abbreviations and Acronyms

<b>CAD</b>	coronary artery disease
<b>CRISPR</b>	clustered regularly interspaced short palindromic repeats
<b>FES</b>	FES proto-oncogene, tyrosine kinase
<b>FURIN</b>	FES upstream region
<b>GWAS</b>	genome-wide association studies
<b>LD</b>	linkage disequilibrium
<b>PRDM1</b>	PR/SET Domain 1
<b>SMA</b>	smooth muscle $\alpha$ -actin
<b>SMC</b>	smooth muscle cell
<b>SNPs</b>	single-nucleotide polymorphisms

locus are the functional variant(s). These SNPs reside within, or in proximity to, the *FURIN* (FES upstream region) and *FES* (FES proto-oncogene, tyrosine kinase) genes. The *FURIN* gene encodes the subtilisin-like proprotein convertase *FURIN*, which possesses proteolytic activity to remove the prodomain of its substrate proteins and thereby activates them. Recent studies have shown that the SNP rs17514846 influences *FURIN* expression<sup>4</sup> and that *FURIN* promotes atherogenesis in murine models.<sup>5</sup>

The *FES* gene located at this genetic locus encodes the cytoplasmic protein-tyrosine kinase known as FES that has been implicated in the regulation of various cellular functions including cell movement, proliferation, differentiation, survival, and inflammation.<sup>6–12</sup> Specifically, it

has been shown to affect leukocyte extravasation,<sup>6,7,11,12</sup> which is an important feature of atherosclerotic plaque development.<sup>13</sup> However, it is unknown whether FES has any involvement in atherosclerosis.

Therefore, in the present study, we sought to investigate if, and which, CAD-associated variants at the 15q26.1 locus modulate *FES* expression and if FES affects atherosclerotic plaque development and composition.

## METHODS

### Data Availability

The data that support the findings of this study are available from the corresponding author upon reasonable request. The methods used are briefly described below, with further details in the online [Supplemental Material](#).

### Bioinformatics Analysis

Information of DNase I hypersensitivity footprints and histone modification marks was from <https://genome.ucsc.edu/> and <https://epgg-test.wustl.edu/browser/>. Data of LD between rs17514846 and other SNPs were from LDlink (<https://ldlink.nci.nih.gov/?tab=ldproxy>). RegulomeDB ranks were from <http://www.regulomedb.org/>. Expression quantitative trait loci data were from the cited references, HaploReg, and the GTEx Portal (<https://www.gtexportal.org/home/>).

### Cells

Under University of Leicester Medicine and Biological Sciences Research Ethics Committee approval, monocytes were isolated from peripheral blood of healthy donors using

the density gradient centrifugation and CD14 positive selection method. THP-1 and RAW264.7 monocytic cells were from the American Type Culture Collection. Primary human coronary artery smooth muscle cells (SMCs) were from Cell Applications.

### CRISPR-Mediated Genome Editing

CRISPR (clustered regularly interspaced short palindromic repeats)-mediated genome editing of THP-1 monocytes was conducted to generate isogenic cells with either the C/C or A/A genotype of rs17514846 and isogenic cells with either the A/A or G/G genotype of rs1894401.

### Electrophoretic Mobility Shift Assay and Super-Shift Assay

An electrophoretic mobility shift assay was performed using oligonucleotide probes corresponding to either the C or A allele of rs17514846 and nuclear protein extracts from THP-1 cells. An electrophoretic mobility super-shift assay was performed using oligonucleotide probes corresponding to either the A or G allele of rs1894401, nuclear protein extracts from THP-1 cells, and an anti-PRDM1 (PR/SET Domain 1) antibody.

### Chromatin Immunoprecipitation Assay

Chromatin immunoprecipitation was performed on THP-1 cells with an anti-PRDM1 antibody (or an isotype control) or with an anti-H3K9ac antibody (or an isotype control), followed by quantitative PCR analysis of the DNA sequence containing and surrounding the rs1894401 site.

### Luciferase Reporter Gene Assay

Two plasmid constructs were generated by inserting a DNA fragment corresponding to a 152bp sequence containing and surrounding the SNP rs1894401 site (with either A or G at the rs1894401 site) into the pGL3-Control Vector. These constructs were individually mixed with a pRL-TK plasmid and then used to transfect RAW264.7 cells, followed by luciferase activity assay.

### CRISPR-Mediated or siRNA-Mediated Gene Knockdown

THP-1 2×Cas9 cells generated by lentiCas9-Blast infection of THP-1 cells were infected with lentiviruses expressing either single guide RNAs (sgRNA) targeting *PRDM1* or scramble sgRNA. *PRDM1* knockdown was verified by immunoblot analysis (Figure S1). Primary human blood monocytes, THP-1 cells, and primary human coronary artery SMCs were transfected with either *FES* small interfering RNA (siRNA) or control siRNA. *FES* knockdown was verified by immunoblot analysis (Figure S2A, S2B, and S2C).

### RT-PCR Analysis

Reverse transcription (RT)-PCR analysis was performed to measure *FES* expression in THP-1 cells with or without *PRDM1* knockdown and *FES* expression in a collection<sup>14</sup> of primary human umbilical vein endothelial cells.

### Immunoblot Analysis

Immunoblot analysis of *FES* was performed with protein lysates from parental THP-1 cells, THP-1 isogenic cells generated by CRISPR-mediated genome editing, THP-1 2×Cas9 cells transfected with *PRDM1* sgRNAs or scramble sgRNA, primary human blood monocytes transfected with *FES* siRNA or control siRNA, THP-1 cells transfected with *FES* siRNA or control siRNA, and lung tissues of *Fes*<sup>-/-</sup>/*ApoE*<sup>-/-</sup> and *Fes*<sup>+/-</sup>/*ApoE*<sup>-/-</sup> mice. *PRDM1* immunoblot analysis was carried out on THP-1 2×Cas9 cells transfected with *PRDM1* sgRNAs or scramble sgRNA.

### Migration, Proliferation, and Apoptosis Assays

Primary human blood monocytes, THP-1 monocytic cells, and human coronary artery SMCs were subjected to a migration assay using trans-wells. Apoptosis assays of primary human blood monocytes and THP-1 monocytic cells were performed with the use of Dead Cell Apoptosis Kit and FITC Annexin V Apoptosis Detection Kit I, respectively. A proliferation assay of THP-1 cells and human coronary artery SMCs was conducted with the use of Cell Counting Kit-8.

### Proteomics and Phosphoproteomics Analyses

Monocytes (THP-1) transfected with either *FES* siRNA or control siRNA were subjected to quantitative proteomics and phosphoproteomics analysis. The motif-x algorithm was used to identify motifs enriched within a set of phosphosites.<sup>15</sup> WebLogo<sup>16</sup> was used to build the motif figures. To predict kinase-substrate relationships, all identified tyrosine, serine, and threonine phosphorylation sites (pY/S/T/) were scored with the NetPhorest algorithm.<sup>17</sup> A pathway enrichment analysis was conducted on proteins that showed differences in modification between cells with siRNA-mediated *FES* knockdown and cells transfected with the control siRNA (Table S1), using Gene Ontology (<http://geneontology.org>).

### Single-Cell RNA-Sequencing of Human Atherosclerotic Plaques

The study was approved by the Medical Ethical Committees of University Medical Center Utrecht and all participants provided informed consent. Human carotid atherosclerotic plaque samples (n=18) from the Athero-Express Biobank<sup>18</sup> were subjected to single-cell RNA-sequencing as previously described.<sup>19</sup> Single-cell RNA-sequencing data were analyzed with the use of SEURAT (<http://www.satijalab.org/seurat>) employing the global-scaling normalization method to standardize the expression levels of *FES* or *PRDM1* against global gene expression levels in each cell.

### Genotyping and Immunohistochemical Analysis of Human Atherosclerotic Plaques

The study was approved by the East London and City Research Ethics Committee and fully complied with Good Clinical Practice guidelines and Tissue Act regulations. Sections of human coronary atherosclerotic plaques were genotyped for rs17514846 and subjected to immunostaining of CD68<sup>20</sup>

and smooth muscle  $\alpha$ -actin (SMA), double fluorescent immunostaining of FES and Iba1, and double fluorescent immunostaining of FES and SMA. Images of immunostaining were analyzed using Image-Pro Software (Media Cybernetics). The atherosclerotic plaques were classified in accordance with standard American Heart Association definition and classification.<sup>21</sup>

## Animal Study

The study was conducted in accordance with the UK Animals (Scientific Procedures) Act 1986, under a Home Office Project License (60/4332) and following the guidelines of ARRIVE (Animal Research: Reporting of In Vivo Experiments). *Fes*<sup>-/-</sup> mice<sup>22</sup> were backcrossed onto a C57BL6/J background for 7 generations before being intercrossed with *Apoe*<sup>-/-</sup> mice (B6.129P2-*Apoe*<sup>tm1Unc</sup>/J) to generate *Fes*<sup>-/-</sup>/*Apoe*<sup>-/-</sup> mice and *Fes*<sup>+/+</sup>/*Apoe*<sup>-/-</sup> control littermates for the study of atherosclerosis. *Fes*<sup>+/+</sup>/*Apoe*<sup>-/-</sup> were excluded from this study. The study was performed only with males, as it has been reported previously that atherosclerotic plaques develop more reproducibly and with less biological variability in male *Apoe*<sup>-/-</sup> mice than in female *Apoe*<sup>-/-</sup> mice.<sup>23,24</sup> Male *Fes*<sup>-/-</sup>/*Apoe*<sup>-/-</sup> mice and male *Fes*<sup>+/+</sup>/*Apoe*<sup>-/-</sup> control littermates were fed a high fat diet for 12 weeks from 6 weeks of age. Lipid levels in fasted blood samples were measured. Aortic root sections were subjected to hematoxylin/eosin staining, immunostaining for monocytes/macrophages (MOMA2) and SMCs (SMA) respectively, and Masson's trichrome staining.

## Statistical Analyses

Statistical analyses were performed with the use of SPSS version 27 and GraphPad Prism version 9.4.1. The Mann-Whitney test or Kruskal-Wallis test (with multiple comparisons adjusting for the number of comparison) was used to ascertain differences between experimental groups in band intensity (after being standardized against  $\beta$ -actin band intensity) in immunoblot analyses, results of migration and proliferation assays of THP-1 and human coronary artery SMCs, and measurements of atherosclerotic lesions and lipid levels in the animal study. The Wilcoxon matched-pairs signed-rank test was performed to ascertain differences in migration and apoptosis between primary human blood monocytes from different individuals transfected with either *FES* siRNA or control siRNA. The *t*-test was used to ascertain a between-genotype difference in FES level in monocytes/macrophages in human coronary atherosclerotic plaques. Linear regression analyses were performed with the independent variable being the rs17514846 C/C, C/A, and A/A genotypes coded as 0, 1, and 2, respectively, and the dependent variable being monocyte/macrophage abundance index, SMC content, or macrophage/SMC ratio, in human coronary atherosclerotic plaques, adjusting for lesion types defined according to the American Heart Association Histological Classification of Atherosclerotic Lesions.<sup>21</sup> The human coronary atherosclerotic plaque collection had  $n \geq 10$  for each of the rs17514846 genotypes (C/C, C/A, and A/A, respectively), with 80% power to detect a genotypic effect size of 0.2 at  $\alpha = 0.05$ .

## RESULTS

### Effect of 15q26.1 Variants on FES Expression in Monocytes

A bioinformatics analysis showed that the GWAS lead CAD-associated SNP rs17514846<sup>1</sup> at the 15q26.1 locus was in high LD ( $r^2 \geq 0.8$ ) with 7 other SNPs in Europeans and South Asians, in high LD ( $r^2 \geq 0.8$ ) with 10 other SNPs in East Asians, but not in high LD with any other SNP in Africans (Figure 1). rs17514846 resides in a transcriptionally active region, with DNase I hypersensitivity footprints and histone acetylation (H3K27ac) marks, while 5 other SNPs (rs2071382, rs11539637, rs7183988, rs7177338, and rs1894401) are in another transcriptionally active region with DNase I hypersensitivity and H3K27ac signatures (Figure 1). rs1894401 has a RegulomeDB rank of 1b, which is higher than the RegulomeDB ranks of the other SNPs in high LD with rs17514846 (Figure 1), indicating that rs1894401 has a greater likelihood to be a regulatory SNP than the others in this group of SNPs. Furthermore, rs17514846 and rs1894401 have been shown to have an expression quantitative trait loci effect on *FES* expression in monocytes and vascular SMCs<sup>25–27</sup> (Figure 1).

To investigate whether rs17514846 and/or rs1894401 can directly modulate FES expression, we conducted CRISPR-mediated genome editing to generate isogenic monocyte cell lines that differed only at the rs17514846 site or at the rs1894401 site, which were otherwise genetically identical. We then performed immunoblot analysis to determine FES levels in these isogenic cell lines. The analysis showed that cells of the rs17514846 A/A genotype (the CAD risk genotype<sup>1,2</sup>) had lower FES levels than cells of the rs17514846 C/C genotype (Figure 2A), while cells of the rs1894401 G/G genotype (in high LD with rs17514846 A/A) had lower FES levels than cells of the rs1894401 A/A genotype (Figure 2B), suggesting that both rs17514846 and rs1894401 directly modulate FES expression.

Electrophoretic mobility shift assays showed that the DNA sequences containing the rs17514846 and rs1894401 sites, respectively, interacted with nuclear proteins. With respect to rs17514846, probes for the C and A alleles both showed interactions with monocyte nuclear proteins of unknown identities, with similar DNA-protein complex bands (Figure S3). Regarding rs1894401, the A and G allele probes produced different DNA-protein complexes, with one of the strong bands being more readily detectable in the assay using the G allele probe than in the assay using the A allele probe (Figure 3A, the DNA-protein complex band indicated by the red arrowhead had higher intensity in lane 4 than in lane 2).

As the G allele of rs1894401 has a greater similarity to the consensus DNA sequence (RRRRAGKGAACKR<sup>28</sup>)

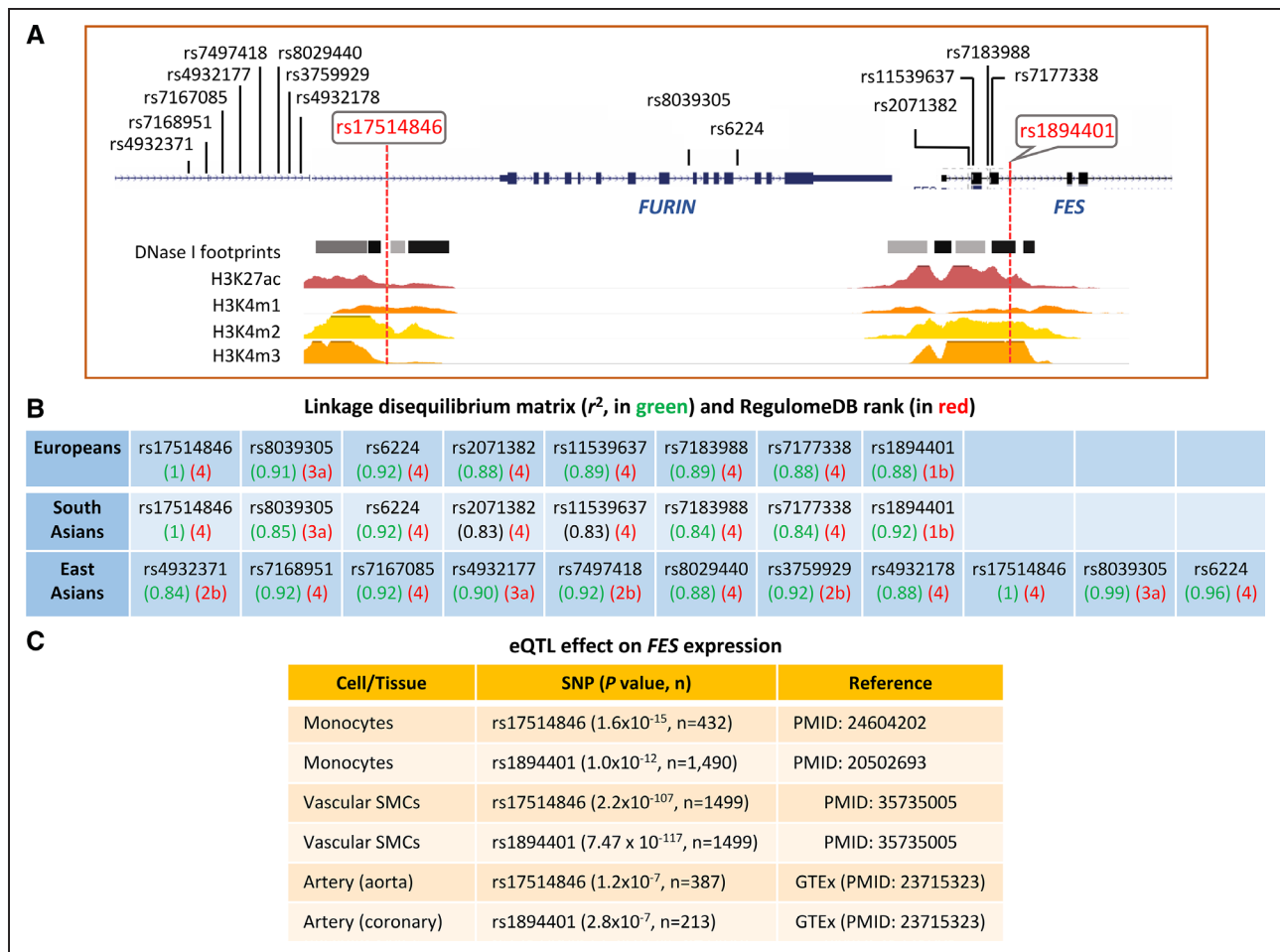


**Figure 1. Results of bioinformatics analysis of the coronary artery disease (CAD) risk locus on chromosome 15q26.1.**

**A**, Illustration of the locations of rs17514846 and single-nucleotide polymorphisms (SNPs) in linkage disequilibrium with rs17514846 at the 15q26.1 locus, and transcriptionally active regions indicated by DNase I hypersensitivity and histone modification marks in monocytes, identified by the ENCODE Project and the Roadmap Epigenomics Project. **B**, Allelic association ( $r^2$ ) between the genome-wide association studies (GWAS) lead SNP rs17514846 and other SNPs in Europeans, South Asians, and East Asians, are indicated in green. Indicated in red are RegulomeDB ranks (\*Definition by RegulomeDB: 1b=eQTL+TF binding+motif+DNase Footprint+DNase peak; 2b=TF binding+any motif+DNase Footprint+DNase peak; 4=TF binding+DNase peak; 3a=TF binding+any motif+DNase peak; 4=TF binding+DNase peak). **C**, Selected eQTL data from Fairfax et al,<sup>25</sup> Zeller et al,<sup>27</sup> Solomon et al,<sup>27</sup> and GTEx (<https://gtexportal.org/home/>). eQTL indicates expression quantitative trait loci; FES, FES proto-oncogene, tyrosine kinase; FURIN, FES upstream region; TF, transcription factor; and SMA, smooth muscle  $\alpha$ -actin.

for the binding site of the transcription factor PRDM1 (also known as BLIMP-1) than the A allele (Figure 3A), we performed a super-shift assay using an anti-PRDM1 antibody to determine whether the nuclear protein giving rise to the above-described band preferentially interacts with the G allele was PRDM1. The super-shift assay demonstrated that the presence of the anti-PRDM1 antibody reduced the intensity of this DNA-protein complex band (Figure 3A, the DNA-protein complex band indicated by the red arrowhead had lower intensity in lane 9 than in lane 4) and brought about a super-shifted DNA-protein complex indicated by the green arrowhead in Figure 3A (lane 9). Taken together, these results suggest that PRDM1 can interact with the rs1894401 site with a preference for the G allele. Interestingly, we observed that *PRDM1* was expressed in monocytes/macrophages in human atherosclerotic plaques (Figure S4).

Furthermore, we performed a chromatin immunoprecipitation assay on monocytes with the use of an anti-PRDM1 antibody. The assay confirmed binding of PRDM1 to the rs1894401 site (Figure 3B). Additionally, we carried out a luciferase reporter assay in which monocytes were transfected with a plasmid vector containing the rs1894401 site and a luciferase reporter gene, together with either a PRDM1 expressing vector or an empty control vector. The assay demonstrated that cotransfection of the PRDM1 expression vector resulted in decreased luciferase activity (Figure 3C), suggesting that PRDM1 reduces the transcription regulatory activity of the rs1894401 site.

Previous studies have reported that PRDM1 can repress the expression of several genes by inducing histone H3 deacetylation, histone H3 methylation, and DNA methylation.<sup>29–33</sup> Therefore, we investigated if PRDM1

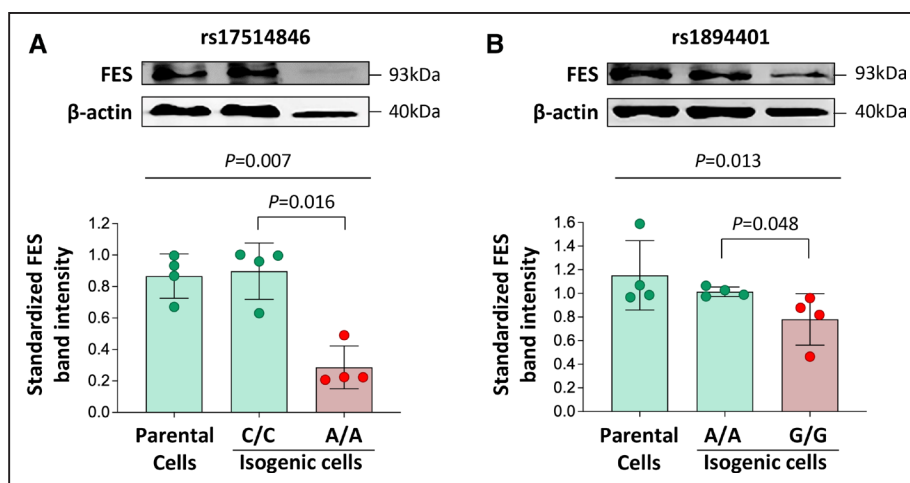


**Figure 2. Differences in FES (FES proto-oncogene, tyrosine kinase) expression level between isogenic monocyte cell lines generated by CRISPR (clustered regularly interspaced short palindromic repeats)-mediated genome editing.**

Human THP-1 monocyte cells were subjected to CRISPR-mediated genome editing to generate isogenic cells of the C/C genotype and isogenic cells of the A/A genotype, respectively, of rs17514846 (A) or isogenic cells of the A/A and G/G genotypes, respectively, of rs1894401 (B). FES levels in the isogenic cell lines were determined by immunoblot analysis. Average representative immunoblot images (top); FES band intensities standardized against band intensities of the reference protein β-actin (bottom). Columns and error bars indicate mean±SD values from n=4 per group; P values from Kruskal-Wallis test with multiple comparisons adjusting for the number of comparison.

affects the histone H3 acetylation status at the *FES* locus. A chromatin immunoprecipitation analysis showed that knockdown of PRDM1 in monocytes increased the histone H3 acetylation level in the chromatin containing the *FES* gene (Figure 3D). Furthermore, a bioinformatics analysis showed that compared with the rs1894401 A allele, the rs1894401 G allele has a lower histone H3 acetylation level, a higher histone H3 methylation level, and a higher chromatin-DNA methylation level, in blood cells (Figure S5).

To investigate whether PRDM1 can influence *FES* expression, we performed RT-PCR and immunoblot analyses to compare *FES* mRNA and FES protein levels between monocytes with PRDM1 knockdown and monocytes without PRDM1 knockdown. The analyses showed that PRDM1 knockdown resulted in higher *FES* mRNA and FES protein levels (Figure 3E), indicating an inhibitory effect of PRDM1 on *FES* expression.

### Effect of FES on Monocyte Behavior

To test whether FES can affect monocyte behavior, we conducted siRNA-mediated knockdown of FES in primary human blood monocytes, and then performed trans-well migration and apoptosis assays. The experiments showed that FES knockdown promoted migration of blood monocytes (Figure 4A) and that blood monocytes with FES knockdown had a tendency toward a reduced death rate (Figure 4B). Additionally, trans-well migration and apoptosis assays of THP-1 monocyte cells demonstrated that FES knockdown promoted migration (Figure S6A) and reduced apoptosis and death (Figure S6B).

Furthermore, we investigated whether FES might influence monocyte proliferation. Since primary blood monocytes generally do not proliferate, we carried out a proliferation assay of human THP-1 monocyte cells transfected with either *FES* siRNA or control siRNA. The assay showed that FES knockdown promoted proliferation of THP-1 monocyte cells (Figure S6C).

Moreover, migration assays of isogenic monocyte cells showed that cells of the rs17514846 A/A genotype (the CAD risk genotype<sup>1,2</sup>) had greater migratory activity than cells of the rs17514846 C/C genotype (Figure 4C), while cells of the rs1894401 G/G genotype (in high LD with rs17514846 A/A) had higher migratory activity than cells of the rs1894401 A/A genotype (Figure 4D).

### Effect of FES on Protein Phosphorylation

Since FES is known to be a protein-tyrosine kinase,<sup>7</sup> we wondered whether FES knockdown could lead to changes in phosphorylation of certain proteins. Therefore, we performed a phosphoproteomics analysis of monocytes transfected with either *FES* siRNA or negative control siRNA. The analysis detected phosphorylation of tyrosine (Y), serine (S), and threonine (T), with the respective phosphorylation motifs shown in Figure 5A. Differences in phosphorylation of 29 proteins were detected between cells with FES knockdown and cells transfected with the negative control siRNA (Figure 5B; Table S1), many of which have previously been implicated in cell migration and proliferation (Columns D and E in Table S1). A functional pathway analysis of these 29 proteins showed

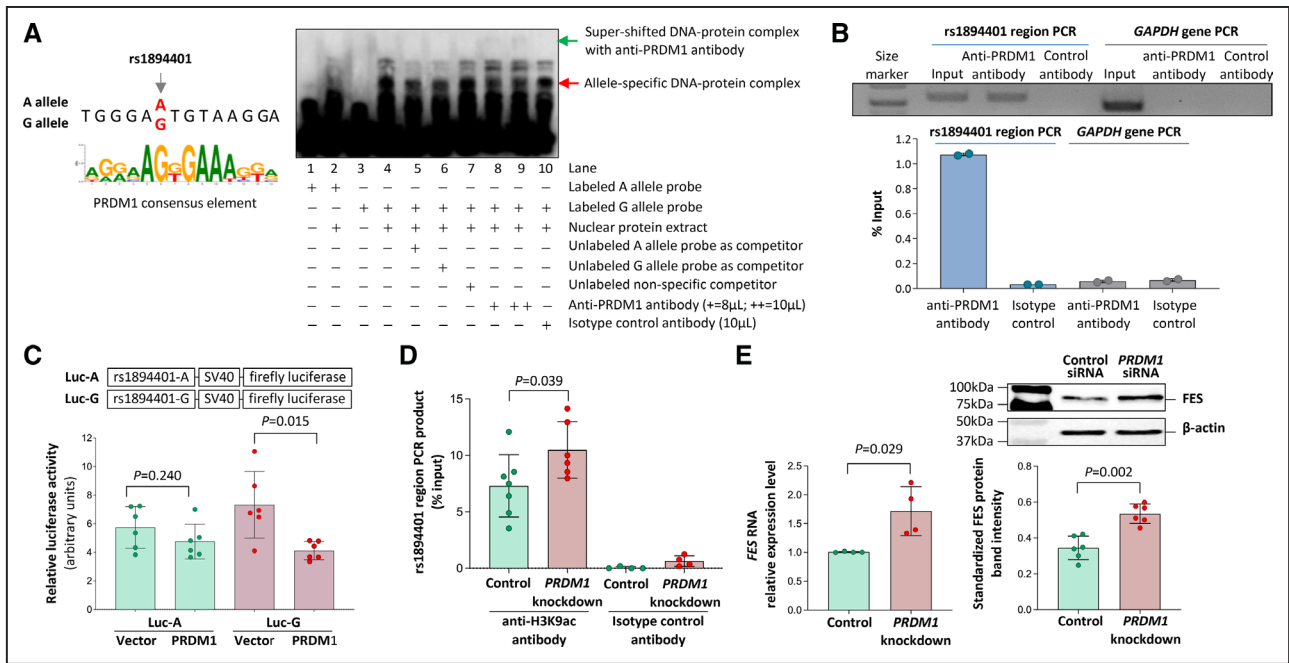


**Figure 3. Interaction of the rs1894401 site with the transcription factor PRDM1 (PR/SET Domain 1).**

**A, Left**, The G allele of rs1894401 has a greater similarity to the consensus DNA sequence for PRDM1 binding<sup>28</sup> than the A allele. **Right**, An average representative image of electrophoretic mobility super-shift assay of THP-1 monocytic cells using probes corresponding to either the A or G allele and an anti-PRDM1 antibody. **B**, Results of chromatin immunoprecipitation analysis of PRDM1. **Top**, Image of gel electrophoresis of PCR products of the rs1894401 region and the *GAPDH* gene (serving as a control), respectively, from input DNA, anti-PRDM1 antibody immunoprecipitated DNA, or isotype control antibody immunoprecipitated DNA. **Bottom**, the amounts of PCR products from immunoprecipitated DNA as compared to amounts of PCR products from input DNA, determined by quantitative PCR analysis. **C**, Results of luciferase assay. Two plasmids containing DNA sequences (152bp) corresponding to either the A or G allele of rs1894401 followed by a firefly luciferase reporter gene were generated. Each of these plasmids, together with a plasmid containing a *Renilla* luciferase gene to serve as a transfection efficiency reference, was transfected into macrophages (Raw 264.7 cells), followed by dual luciferase assays. Data shown are mean ( $\pm$ SD) of standardized firefly luciferase activity (the ratio of firefly luciferase activity over *Renilla* luciferase activity),  $n=6$  per group,  $P$  values from 2-tailed Mann-Whitney test. **D**, THP-1 monocytic cells with and without PRDM1 knockdown (knockdown of PRDM1 is shown in Figure S1) were subjected to chromatin immunoprecipitation with either an anti-H3K9ac antibody or an isotype control antibody, followed by a quantitative PCR analysis of the rs1894401 region. Data shown are mean ( $\pm$ SD) of the amounts of PCR products from DNA immunoprecipitated with the anti-H3K9ac antibody or the isotype control antibody, relative to the amounts of PCR products from input DNA;  $n=4-7$  per group;  $P$  value from 2-tailed Mann-Whitney test. **E**, Results of *FES* (*FES* proto-oncogene, tyrosine kinase) reverse transcription (RT)-PCR (**left**) and *FES* immunoblot analysis (**right**) of THP-1 cells with and without PRDM1 knockdown (knockdown of PRDM1 is shown in Figure S1). **Left**, Mean ( $\pm$ SD) of *FES* RNA levels relative to *ACTB* RNA level, determined by the  $\Delta$ Ct method;  $n=4$  per group;  $P$  value from 2-tailed Mann-Whitney test. **Top right**, Average representative immunoblot images. **Bottom right**, Mean ( $\pm$ SD) of *FES* protein band intensities standardized against band intensities of the reference protein  $\beta$ -actin, from  $n=6$  per group;  $P$  value from 2-tailed Mann-Whitney test.

enrichment of pathways involved in RHOBTB/RHBTB2 GTPase cycles, RNA polymerase II transcription termination, and mRNA processing (Figure 5B; Table S2).

### Effect of 15q26.1 Variant on FES Expression and Monocyte/Macrophage Abundance, in Human Atherosclerotic Plaques

An analysis of data from a single-cell transcriptomics study of human atherosclerotic plaques showed that in atherosclerotic plaques, cells that expressed *FES* were predominately monocytes/macrophages, although several other cell types including SMCs and endothelial cells also expressed *FES* (Figure 6A). The average level of *FES* expression in monocytes/macrophages that expressed this gene was 1.47-fold higher

( $P=2.9 \times 10^{-40}$ ), compared with the average level of *FES* expression in all other cell types that expressed it (Figure 6A).

Double immunostaining of *FES* and the monocyte/macrophage marker Iba1 confirmed that monocytes/macrophages in atherosclerotic plaques contained *FES* (Figure 6B). In an analysis of a collection of human coronary atherosclerotic plaques from different individuals, we observed that *FES* levels in monocytes/macrophages were lower in atherosclerotic plaques from patients of the rs17514846 A/A genotype (in LD with the rs1894401 G/G genotype) than in plaques from patients of the rs17514846 C/C genotype (Figure 6B). Furthermore, we found that plaques from patients of the rs17514846 A/A genotype had a greater abundance of monocytes/macrophages than plaques from patients of the C/C genotype (Figure 7).

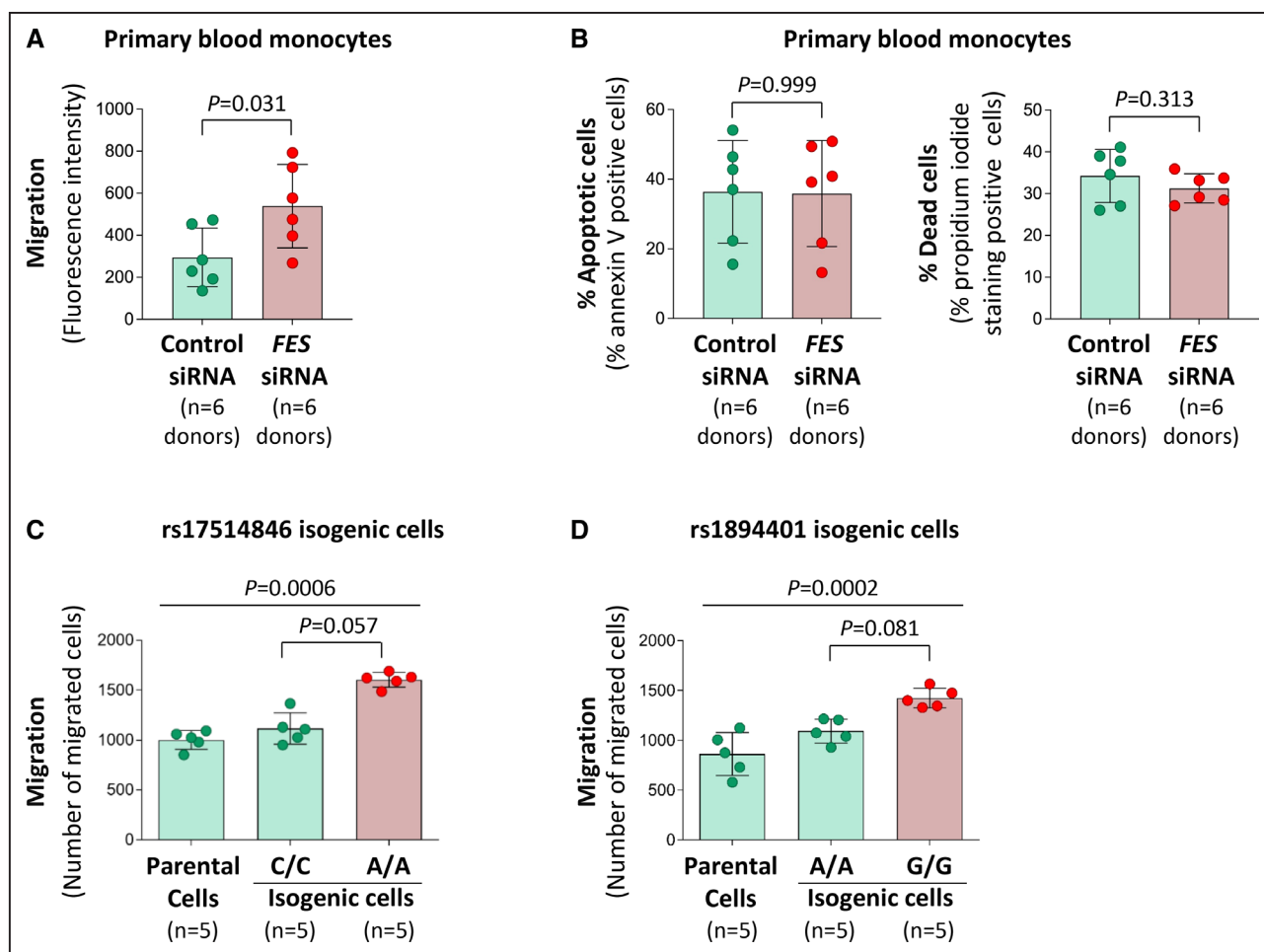


**Figure 4. Effects of FES (FES proto-oncogene, tyrosine kinase) knockdown, rs17514846, and rs1894401 on monocyte behavior.**

**A** and **B**, Human peripheral blood monocytes transfected with either negative control small interfering RNA (siRNA) or *FES* siRNA (knockdown of *FES* is shown in Figure S2A) were subjected to trans-well migration assay (**A**) and apoptosis assay (following incubation with the apoptosis inducer staurosporine for 4 h; **B**), respectively. Columns and error bars represent mean $\pm$ SD; *P* values are from 2-tailed Wilcoxon matched-pairs signed-rank test. **C** and **D**, Results of trans-well migration assays of isogenic monocytic cells of either the rs1894401 C/C or A/A genotype (**C**) and isogenic monocytic cells of either the rs1894401 A/A or G/G genotype (**D**). Columns and error bars represent mean $\pm$ SD; *P* values from Kruskal-Wallis test with multiple comparisons adjusting for the number of comparison.

Previous studies have shown that the CAD-associated variants at the 15q26.1 locus influenced *FES* expression in vascular SMCs.<sup>27,34</sup> Therefore, we investigated *FES* expression in SMCs in human coronary atherosclerotic plaques in relation to the 15q26.1 variant genotype. We detected an association of the rs17514846 A/A genotype (in LD with rs1894401 G/G genotype) with lower *FES* expression in SMCs in atherosclerotic plaques (Figure S7). Additionally, we observed a nonsignificant trend toward a greater SMC content and a higher ratio of monocytes/macrophages versus SMCs, in atherosclerotic plaques from patients of the rs17514846 A/A genotype compared with plaques from patients of the rs17514846 C/C genotype (Figure S8A and S8B). In support, we found that *FES* knockdown promoted migration of cultured primary coronary artery SMCs (Figure S9A), albeit inhibiting proliferation (Figure S9B).

The above-mentioned single-cell transcriptomics analysis of human atherosclerotic plaques showed that

endothelial cells also expressed *FES* (Figure 6A). Therefore, we additionally investigated if the 15q26.1 variant influenced *FES* expression in endothelial cells. However, we detected no significant association between the 15q26.1 variant and *FES* expression in cultured vascular endothelial cells from different individuals (Figure S10).

### Effect of *FES* on Atherosclerotic Plaque Development and Composition, in an Animal Model

To investigate whether *FES* plays a role in atherosclerosis, we tested a possible effect of *Fes* knockout in a well-established mouse model of atherosclerosis. We fed *Fes*<sup>-/-</sup>/*Apoe*<sup>-/-</sup> mice (test group) and *Fes*<sup>+/+</sup>/*Apoe*<sup>-/-</sup> littermates (control group) a high fat diet for 12 weeks from 6 weeks of age and then examined whether atherosclerotic lesions differed between the 2 groups. Analyses of aortic root atherosclerotic sections showed that the *Fes*<sup>-/-</sup>/*Apoe*<sup>-/-</sup> mice



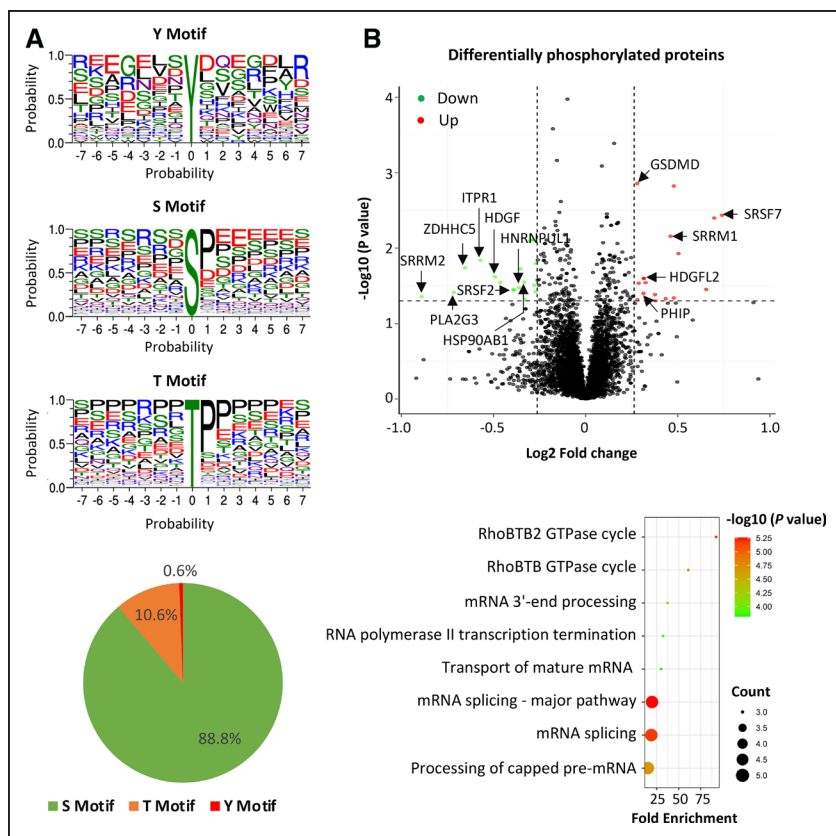


**Figure 5. Results of phosphoproteomics analysis of monocytes with vs without FES (FES proto-oncogene, tyrosine kinase) knockdown.**

**A**, Motifs of phosphorylation of tyrosine (Y), serine (S), and threonine (T), detected. **B, Top**, Volcano plot of proteins (represented by red or green dots) that are differentially phosphorylated in cells with small interfering RNA (siRNA)-mediated FES knockdown compared with cells transfected with a negative control siRNA. **Bottom**, Bubble plot showing pathways with enrichment of proteins that are differentially phosphorylated in cells with siRNA-mediated FES knockdown compared with cells transfected with a negative control siRNA. *P* values are from Fisher exact test implemented with the default setting of Gene Ontology enrichment analysis (<http://geneontology.org>). GSDMD indicates gasdermin D; HDGF, heparin binding growth factor; HDGF2, hepatoma-derived growth factor-related protein 2; HNRNPUL1, heterogeneous nuclear ribonucleoprotein U like 1; HSP90AB1, heat shock protein 90 alpha family class B member 1; ITPR1, inositol 1,4,5-trisphosphate receptor type 1; PHIP, pleckstrin homology domain interacting protein; PLA2G3, phospholipase A2 group III; SRRM1, serine/arginine repetitive matrix 1; SRRM2, serine/arginine repetitive matrix 2; SRSF7, serine/arginine-rich splicing factor 7; and ZDHHC5, zinc finger DHHC-type palmitoyltransferase 5.

had an increase in mean lesion area ( $P=0.007$ ), greater monocyte/macrophage abundance ( $P=0.018$ ), higher SMC content ( $P=0.020$ ), and less collagen ( $P=0.012$ ), as compared with lesions of *Fes*<sup>+/+</sup>/*Apoe*<sup>-/-</sup> littermates (Figure 8A–8D). There was no significant difference between the 2 groups in plasma levels of total cholesterol, very low-density lipoprotein, low-density lipoprotein, high-density lipoprotein, or triglycerides (Figure S11), suggesting that FES does not affect plasma lipid levels.

## DISCUSSION

GWAS have unveiled an association between variants at the 15q26.1 locus and CAD susceptibility.<sup>1,2</sup> Here, we provide several novel insights into the molecular and cellular basis of this association and its translational and clinical relevance, using both human and animal studies. Our findings also provide some more general insights underlying genetic associations with disease.

From a mechanistic perspective, one of the novel findings of our study is that the 15q26.1 locus contains at least 2 functional SNPs, that is, rs17514846 and rs1894401. Our analysis of isogenic monocytic cell lines generated by CRISPR-mediated genome editing showed that the rs17514846-A allele (the CAD risk allele) and the rs1894401-G allele (in high LD with the rs17514846-A allele) both decreased *FES* expression. This finding not only suggests that the association between variants at the

15q26.1 locus and CAD susceptibility is likely to be mediated, at least in part, by reduced *FES* expression but also provides a paradigm that a disease risk locus can harbor >1 functional variant that are in high LD. Thus, a genetic signal can be a composite of 2 or more functional variants in LD, and this needs to be considered as a possibility in studies aimed at identifying the causal variant(s) at disease loci.

Our previous work showed that rs17514846 modulates the expression of *FURIN*, with the rs17514846-A allele having higher *FURIN* expression than the rs17514846-C allele, in monocytes.<sup>4</sup> This and the present study (which shows that rs17514846 affects *FES* expression, with the rs17514846-A allele having lower *FES* expression in monocytes) collectively indicate that the CAD-associated variant at the 15q26.1 locus influences the expression of both the *FURIN* and *FES* genes, but in opposing directions. *FURIN* has been reported to promote atherosclerosis,<sup>5</sup> while our present study shows that *FES* plays a protective role. Taken together, these findings provide another paradigm underpinning GWAS associations; namely, the impact on the disease may be a composite of the impact of a disease-related variant on the expression of >1 gene involved in the disease process.

*FES* is expressed predominately in differentiated myeloid cells.<sup>6</sup> Previous studies have suggested that the regulation of *FES* transcription involves binding sites (located within 150 nucleotides of the transcriptional start site) for the transcription factors Sp1, PU.1/Spi-1,

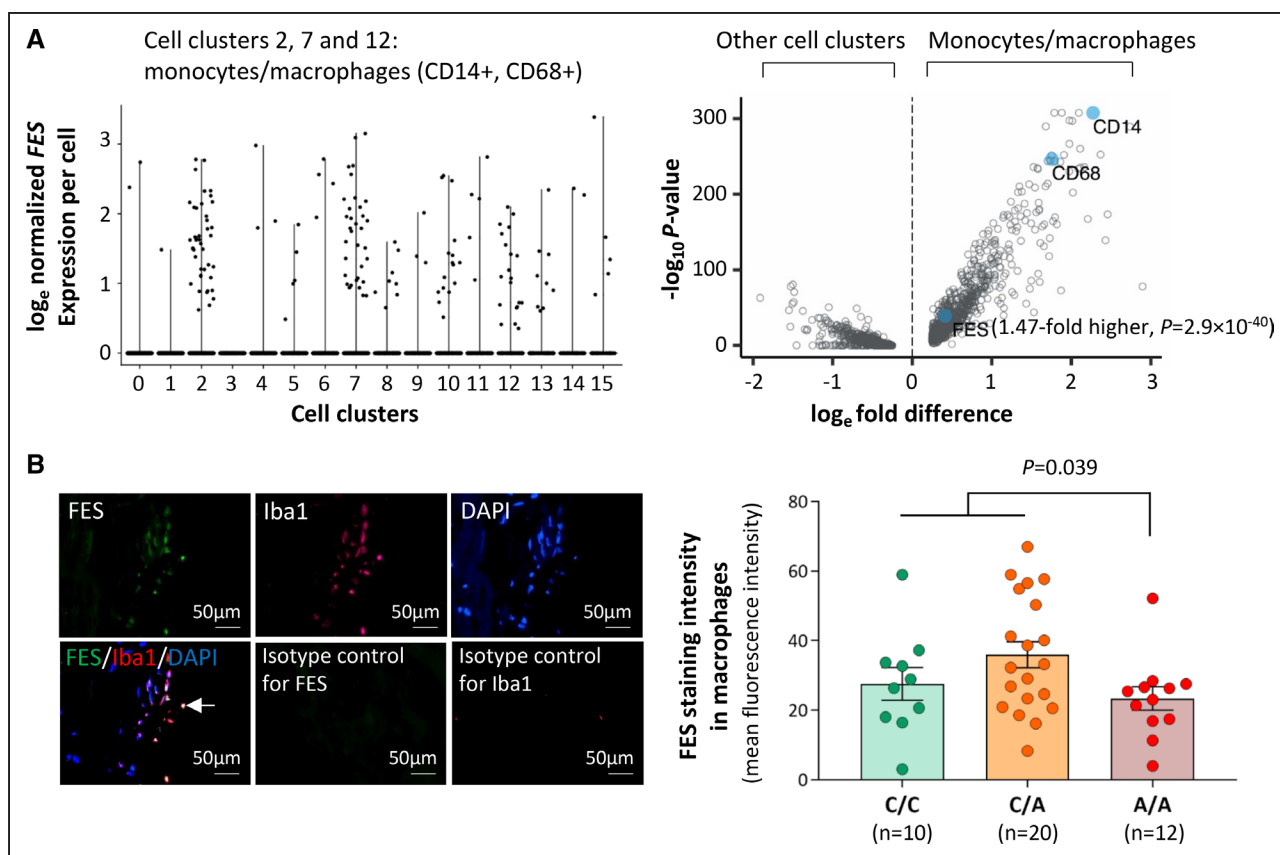


**Figure 6. FES (FES proto-oncogene, tyrosine kinase) expression in monocytes/macrophages in human atherosclerotic plaques.**

**A**, Results of single-cell transcriptomic analysis of human atherosclerotic plaques. **Left**, Graph shows that in atherosclerotic plaques, cells (represented by black dots), which express *FES* are predominantly monocytes/macrophages. The x-axis shows different cell clusters, specifically, 2/7/12: monocytes/macrophages (CD14+, CD68+); 0/1/3/4/5/6/9: T lymphocytes (CD3E+); 8: smooth muscle cells (ACTA2+, MYH11+); 10/13: endothelial cells (CD34+, PECAM1+); 11: B lymphocytes (CD79A+); 15: mast cells (KIT+). The y-axis shows normalized *FES* expression levels with natural logarithm transformation (as described in the [Supplemental Material](#)). **Right**, Graph shows higher *FES* expression in monocytes/macrophages (cell clusters 2/7/12) than in other cell clusters. Each blue closed circle or opened circle symbolizes one gene. The x-axis shows mean  $\log_2$ -transformed, normalized fold differences in gene expression comparing monocytes/macrophages vs all other cell clusters. The y-axis shows  $\log_{10}$ -*P*-values for comparisons between monocytes/macrophages and all other cell clusters in gene expression. **B**, Human coronary atherosclerotic plaques from different individuals were subjected to double fluorescent immunostaining for *FES* and the macrophage marker ionized calcium binding adaptor molecule 1 (*Iba1*). Nuclei were stained with DAPI (4',6-diamidino-2-phenylindole). Fluorescent immunostaining images were analyzed using Image-Pro Plus image analysis software. **Left**, Average representative images. The arrow indicates *FES* and *Iba1* double positive staining; **Right**, *FES* mean fluorescence intensity in macrophages (*Iba1* positive) in atherosclerotic plaques from individuals of the C/C, C/A, and A/A genotypes, respectively. Columns and error bars indicate mean  $\pm$  SEM. Numbers per group are indicated in the figure. The *P* value is from a 2-tailed *t*-test.

and FEF<sup>35–37</sup> a tissue-specific cis-acting repressor element in the first intron,<sup>38</sup> and a putative locus control region at the 5' (promoter-proximal) end of the gene.<sup>39</sup> In the present study, we found that the transcription factor PRDM1 interacted with the rs1894401 site located within a consensus PRDM1 binding element (RRRRAG-KGAAAKKR) in intron 3 of the *FES* gene, giving rise to a DNA-protein complex detected by electrophoretic mobility shift assay. The binding of PRDM1 to the rs1894401 site was confirmed by chromatin immunoprecipitation. Luciferase reporter gene assay further showed that PRDM1 reduced the transcription regulatory activity of the rs1894401 site. These, together with the finding that knockdown of PRDM1 in monocytes resulted in an increase in *FES* mRNA and *FES* protein levels indicate

that PRDM1 also plays a role in the regulation of *FES* expression, exerting a down-regulatory effect on *FES* transcription. Previous studies have shown that PRDM1 can repress the expression of several genes by inducing histone H3 deacetylation, histone H3 methylation, and DNA methylation.<sup>29–33</sup> In the present study, we found that knockdown of PRDM1 increased the histone H3 acetylation level in the chromatin containing the *FES* gene. Furthermore, a bioinformatics analysis showed that compared with the rs1894401 A allele, the rs1894401 G allele has a lower histone H3 acetylation level, a higher histone H3 methylation level, and a higher chromatin-DNA methylation level, in blood cells. These results together suggest that PRDM1 may inhibit *FES* expression by modulating the chromatin containing the *FES* gene.

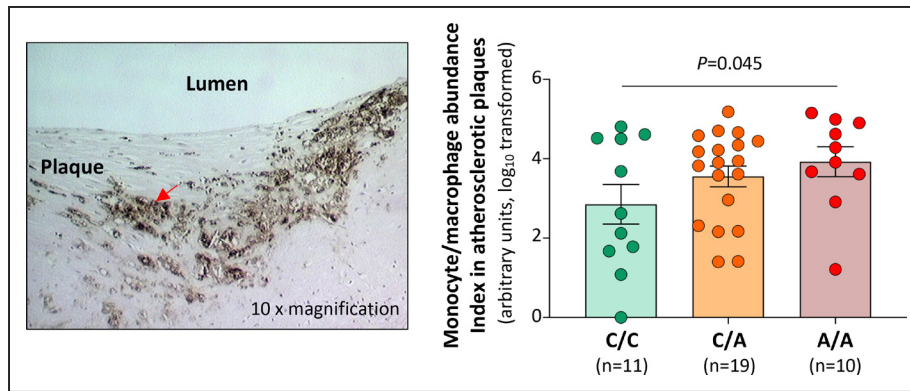


**Figure 7. Monocyte/macrophage abundance in human atherosclerotic plaques by rs17514846 genotype.**

Human coronary atherosclerotic plaques from different individuals were subjected to immunostaining for the monocyte/macrophage marker CD68 and genotyping for single-nucleotide polymorphism (SNP) rs17514846. Immunohistochemical images were analyzed using Image-Pro Plus image analysis software. **Left**, An average representative image of immunostaining at 10× magnification. The arrow indicates CD68-positive staining. **Right**, Monocyte/macrophage abundance indices in atherosclerotic plaques from individuals of the C/C, C/A, and A/A genotypes, respectively. Columns and error bars indicate values of mean±SEM. Numbers of individuals per group are shown in the figure. The *P* value is from a linear regression analysis with the dependent variable being monocyte/macrophage abundance index (normalized by log<sub>10</sub> transformation) and the independent variable being rs17514846 C/C, C/A, and A/A genotypes coded as 0, 1, and 2, respectively, and with adjustment for lesion types defined according to the American Heart Association Histological Classification of Atherosclerotic Lesions.

FES is known to participate in the regulation of inflammation and innate immunity.<sup>6</sup> Previous studies with *Fes*<sup>-/-</sup> mice showed increased leukocyte recruitment and extravasation at sites of inflammation;<sup>12</sup> and *Fes*<sup>-/-</sup> mice were more sensitive to in vivo endotoxin challenge,<sup>22</sup> which was associated with enhanced in vitro activation of NFκB (Nuclear Factor Kappa B)-mediated tumor necrosis factor-α (TNFα) production in bone marrow-derived macrophages and reduced phagocytic activity.<sup>11</sup> In line with the reported finding of increased endotoxin-induced leukocyte recruitment in *Fes*<sup>-/-</sup> mice,<sup>12</sup> our study showed that atherosclerotic lesions in *Fes*<sup>-/-</sup>/*Apoe*<sup>-/-</sup> mice had higher a monocyte/macrophage abundance and that knockdown of FES promoted migration of primary human blood monocytes. Additionally, we found that FES knockdown induced proliferation of monocytic cells (THP-1 cells).

Mechanistic studies have previously described roles for FES in signaling downstream from receptor systems including those for cytokines and growth factors,<sup>40,41</sup> extracellular matrix ligands,<sup>42</sup> and adherens junction cell-cell interactions.<sup>43</sup> Although FES is known to function as a nonreceptor protein-tyrosine kinase, its substrates have not been comprehensively described. Our phosphoproteomics analysis identified 29 proteins differentially phosphorylated in monocytes with siRNA-mediated FES knockdown as compared with monocytes transfected with the negative control siRNA. The detected differential phosphorylation sites, however, are serine residues and thus not direct FES targets. It is possible that FES indirectly influences the phosphorylation of these proteins by interacting with 1 or more unknown serine kinases. Interestingly, several of the differentially phosphorylated proteins (including SRRM1 [Serine/Arginine Repetitive Matrix 1], SRRM2 [Serine/Arginine Repetitive Matrix 2], SRSF7 [Serine/Arginine-Rich Splicing Factor

7; also named SFRS7], ITPR1 [Inositol 1,4,5-Trisphosphate Receptor Type 1], and BICD2 [Bicaudal D Homolog 2]) detected in our study have been reported to be differentially phosphorylated by blocking ErbB2 receptor tyrosine kinase,<sup>44</sup> suggesting that FES and ErbB2 receptor tyrosine kinase could potentially work in concert.

A functional pathway analysis of the differentially phosphorylated proteins detected in this study showed enrichment of pathways involved in RhoBTB/RhoBTB2 GTPase cycle and mRNA processing, respectively. Noticeably, previous studies have demonstrated that FES can activate Rho family GTPases,<sup>45,46</sup> and there is substantial evidence showing that the RhoBTB proteins play a role in regulating cell mobility, growth, and apoptosis.<sup>47,48</sup> Taken together, the findings from this and the previous studies suggest that FES could influence cell behavior via Rho GTPase-mediated pathways.

Most of the proteins, which our study observed differential phosphorylation of monocytes with siRNA-mediated FES knockdown as compared with monocytes transfected with the negative control siRNA, have been previously implicated in cell migration and/or proliferation, as annotated in Table S2. Therefore, it is plausible that FES can influence monocyte behavior by modulating the posttranslational modifications of many different proteins.

In line with the in vitro finding that the CAD-associated variants at the 15q26.1 locus promote monocyte migration, we observed that ex vivo coronary atherosclerotic plaques from patients of 15q26.1 CAD risk genotype had a greater monocyte/macrophage abundance. There was also a trend toward a higher monocyte/SMC ratio in plaques from patients carrying the risk allele, but this was statistically nonsignificant, which could possibly be due to the moderate sample size not providing sufficient statistical power and/or due to the risk allele also increasing

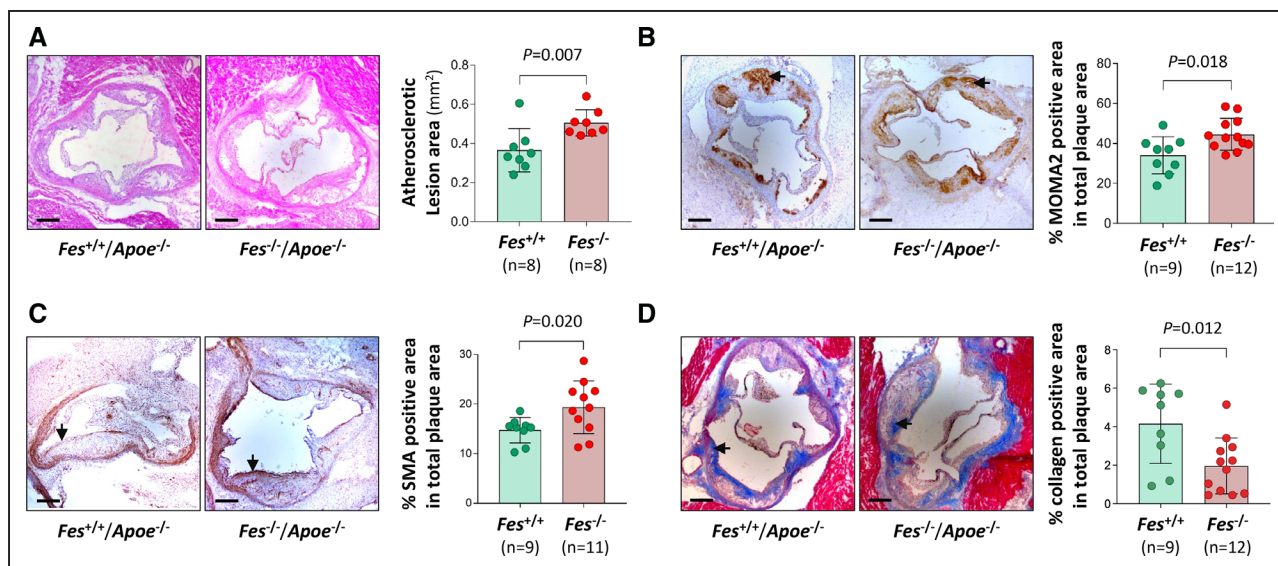


**Figure 8. Differences between *Fes*<sup>-/-</sup>/*Apoe*<sup>-/-</sup> mice and *Fes*<sup>+/+</sup>/*Apoe*<sup>-/-</sup> mice in atherosclerotic lesion size and composition.**

*Fes*<sup>-/-</sup>/*Apoe*<sup>-/-</sup> mice and *Fes*<sup>+/+</sup>/*Apoe*<sup>-/-</sup> littermates were fed a high fat diet for 12 weeks from 6 weeks of age. Thereafter, aortic root sections were subjected to hematoxylin/eosin staining (A), immunostaining for monocytes/macrophages (MOMA2) (B), immunostaining for smooth muscle cells (SMA) (C), and Masson trichrome staining for collagen (D). Morphometric quantification was performed with the use of Fiji software. Arrows indicate stain-positive areas. Bars, 200  $\mu$ m. Mean (SD) values in the *Fes*<sup>-/-</sup>/*Apoe*<sup>-/-</sup> group and the *Fes*<sup>+/+</sup>/*Apoe*<sup>-/-</sup> group, respectively, were 0.505 (0.067) mm<sup>2</sup> and 0.365 (0.111) mm<sup>2</sup> for atherosclerotic lesion area in the aortic root sections (A), 44.52% (7.97%) and 34.02% (9.25%) for MOMA2 positive stain area (B), 19.36% (5.32%) and 14.73% (2.57%) for SMA positive stain area (C), and 1.97% (1.45%) and 4.16% (2.06%) for collagen positive stain area (D). Numbers per group are shown in the figure. *P* values are from 2-tailed Mann-Whitney test.

SMC abundance in atherosclerotic plaques. Pertaining to the latter, our study showed an influence of FES on vascular SMCs migration in vitro and an increase of SMC content in atherosclerotic lesions in *Fes* knockout mice.

To our knowledge, our study is the first to show an involvement of FES in atherosclerosis. Using a well-established mouse model, we found that *Fes* knockout was associated with the development of larger atherosclerotic lesions, indicating that FES plays a protective role against atherogenesis. Additionally, we found that atherosclerotic plaques in *Fes*<sup>-/-</sup>/*Apoe*<sup>-/-</sup> mice had a greater abundance of monocytes/macrophages and SMCs, both of which are well-established players in atherogenesis.

Our study shows that human atherosclerotic lesions express *PRDM1*. Studies by other investigators have demonstrated that attenuating *PRDM1* in B cells inhibited atherosclerosis development in mouse models.<sup>49</sup> In light of the findings of our study, which shows that *PRDM1* represses FES expression and that FES inhibits atherosclerosis, it is plausible that *PRDM1* could promote atherosclerosis partly via reducing FES expression, which warrants separate detailed investigations beyond the scope of the present study.

Our study included a series of in vitro, ex vivo as well as in vivo experiments, which provide complementary evidence of an influence of the 15q26.1 variants on FES expression and a role played by FES in atherosclerosis. This represents one of the strengths of this work. However, no correction of *P*-values for multiple

testing was carried out, which may be considered a limitation of this study.

In summary, our study shows that FES influences migration of monocytes and vascular SMCs, with a protective effect against atherosclerosis, and that the CAD risk variants at the 15q26.1 locus reduce FES expression in monocytes and increase monocyte/macrophage abundance in atherosclerotic plaques. These findings provide a better understanding of the mechanism underlying the link between the 15q26.1 locus and CAD susceptibility and suggest that modulation of FES expression or its function may prove useful for CAD intervention.

## ARTICLE INFORMATION

Received April 20, 2022; revision received October 16, 2022; accepted October 17, 2022.

### Affiliations

Department of Cardiovascular Sciences, University of Leicester, and National Institute for Health Research Leicester Biomedical Research Centre, Leicester, United Kingdom (E.K., D.G.M., P.J.S., G.E.M., P.G., P.D.J., T.R.W., E.J.S., N.J.S., S.Y.). Central Diagnostic Laboratory, University of Utrecht, The Netherlands (S.W.v.d.L., G.P.). Cardiovascular Disease Translational Research Programme, Yong Loo Lin School of Medicine, National University of Singapore, Singapore (Y.W., H.Y., S.Y.). Shantou University Medical College, China (W.Y., J.C., S.Y.). William Harvey Research Institute, Queen Mary University of London, United Kingdom (K.C., R.N.P., J.L., X.Z., Q.X.). Department of Human Nutrition, University of Agriculture in Kraków, Poland (R.B.K.). Department of Pathology and Molecular Medicine, Queen's University, Kingston, Canada (P.A.G.).

### Acknowledgments

The authors acknowledge the help and support from the staff of the Division of Biomedical Services, Preclinical Research Facility, University of Leicester, for technical support and the care of experimental animals.

## Sources of Funding

We are thankful for the support of the British Heart Foundation (PG/16/9/31995, RG/16/13/32609, PG/18/73/34059, SP/19/2/344612, and RG/19/9/34655), the National University of Singapore and the National University Health System Internal Grant Funding (NUHSRO/2022/004/Start-up/01), the Netherlands CardioVascular Research Initiative of the Netherlands Heart Foundation (CVON 2011/B019 and CVON 2017-20), the AI for Health working group of the EWUU alliance (<https://aiforhealth.ewuu.nl/>), the European Research Area Network on Cardiovascular Diseases program (01KL1802), the Leducq Foundation, and the National Natural Science Foundation of China (81370202, 82070466, and 82000341). This work falls under the portfolio of research conducted within the National Institute for Health Research Leicester Biomedical Research Centre.

## Disclosures

S.W. van der Laan received funding from Roche for unrelated work. The other authors report no conflicts.

## Supplemental Material

Expanded Methods  
References 14–24  
Figures S1–S13  
Tables S1 and S2

## REFERENCES

- CARDIoGRAMplusC4D Consortium, Deloukas P, Kanoni S, Willenborg C, Farrall M, Assimes TL, Thompson JR, Ingelsson E, Saleheen D, Erdmann J, Goldstein BA, et al. Large-scale association analysis identifies new risk loci for coronary artery disease. *Nat Genet.* 2013;45:25–33. doi: 10.1038/ng.2480
- Nikpay M, Goel A, Won HH, Hall LM, Willenborg C, Kanoni S, Saleheen D, Kyriakou T, Nelson CP, Hopewell JC, et al. A comprehensive 1,000 Genomes-based genome-wide association meta-analysis of coronary artery disease. *Nat Genet.* 2015;47:1121–1130. doi: 10.1038/ng.3396
- van der Harst P, Verweij N. Identification of 64 novel genetic loci provides an expanded view on the genetic architecture of coronary artery disease. *Circ Res.* 2018;122:433–443. doi: 10.1161/CIRCRESAHA.117.312086
- Zhao G, Yang W, Wu J, Chen B, Yang X, Chen J, McVey DG, Andreadi C, Gong P, Webb TR, et al. Influence of a coronary artery disease-associated genetic variant on FURIN expression and effect of furin on macrophage behavior. *Arterioscler Thromb Vasc Biol.* 2018;38:1837–1844. doi: 10.1161/ATVBAHA.118.311030
- Yakala GK, Cabrera-Fuentes HA, Crespo-Avilan GE, Rattanasopa C, Burlacu A, George BL, Anand K, Mayan DC, Corliano M, Hernández-Reséndiz S, et al. FURIN inhibition reduces vascular remodeling and atherosclerotic lesion progression in mice. *Arterioscler Thromb Vasc Biol.* 2019;39:387–401. doi: 10.1161/ATVBAHA.118.311903
- Greer P. Closing in on the biological functions of Fps/Fes and Fer. *Nat Rev Mol Cell Biol.* 2002;3:278–289. doi: 10.1038/nrm783
- Jucker M, McKenna K, da Silva AJ, et al. The Fes protein-tyrosine kinase phosphorylates a subset of macrophage proteins that are involved in cell adhesion and cell-cell signaling. *J Biol Chem.* 1997;272:2104–2109. doi: 10.1074/jbc.272.4.2104
- Cheng HY, Schiavone AP, Smithgall TE. A point mutation in the N-terminal coiled-coil domain releases c-Fes tyrosine kinase activity and survival signaling in myeloid leukemia cells. *Mol Cell Biol.* 2001;21:6170–6180. doi: 10.1128/MCB.21.18.6170-6180.2001
- Yu G, Smithgall TE, Glazer RI. K562 leukemia cells transfected with the human c-fes gene acquire the ability to undergo myeloid differentiation. *J Biol Chem.* 1989;264:10276–10281. doi: 10.1016/S0021-9258(18)81796-3
- Voisset E, Lopez S, Dubreuil P, De Sepulveda P. The tyrosine kinase FES is an essential effector of KITD816V proliferation signal. *Blood.* 2007;110:2593–2599. doi: 10.1182/blood-2007-02-076471
- Parsons SA, Greer PA. The Fps/Fes kinase regulates the inflammatory response to endotoxin through down-regulation of TLR4, NF- $\kappa$ B activation, and TNF- $\alpha$  secretion in macrophages. *J Leukoc Biol.* 2006;80:1522–1528. doi: 10.1189/jlb.0506350
- Parsons SA, Mewburn JD, Truesdell P, Greer PA. The Fps/Fes kinase regulates leucocyte recruitment and extravasation during inflammation. *Immunology.* 2007;122:542–550. doi: 10.1111/j.1365-2567.2007.02670.x
- Gerhardt T, Ley K. Monocyte trafficking across the vessel wall. *Cardiovasc Res.* 2015;107:321–330. doi: 10.1093/cvr/cw147
- Ng FL, Boedtker E, Witkowska K, Ren M, Zhang R, Tucker A, Aalkjær C, Caulfield MJ, Ye S. Increased NBCn1 expression, Na<sup>+</sup>/HCO<sub>3</sub><sup>-</sup> co-transport and intracellular pH in human vascular smooth muscle cells with a risk allele for hypertension. *Hum Mol Genet.* 2017;26:989–1002. doi: 10.1093/hmg/ddx015
- Wagih O, Sugiyama N, Ishihama Y, Beltrao P. Uncovering phosphorylation-based specificities through functional interaction networks. *Mol Cell Proteomics.* 2016;15:236–245. doi: 10.1074/mcp.M115.052357
- Crooks GE, Hon G, Chandonia JM, Brenner SE. WebLogo: a sequence logo generator. *Genome Res.* 2004;14:1188–1190. doi: 10.1101/gr.849004
- Miller ML, Jensen LJ, Diella F, Jørgensen C, Tinti M, Li L, Hsiung M, Parker SA, Bordeaux J, Sicheritz-Ponten T, et al. Linear motif atlas for phosphorylation-dependent signaling. *Sci Signal.* 2008;1:ra2. doi: 10.1126/scisignal.1159433
- Verhoeven BA, Velema E, Schoneveld AH, de Vries JP, de Bruin P, Seldenrijk CA, de Kleijn DP, Busser E, der Graaf YV, Mol F, et al. Athero-express: differential atherosclerotic plaque expression of mRNA and protein in relation to cardiovascular events and patient characteristics. Rationale and design. *Eur J Epidemiol.* 2004;19:1127–1133. doi: 10.1007/s10564-004-2304-6
- Depuydt MAC, Prange KHM, Slenders L, Örd T, Elbersen D, Boltjes A, De Jager SC, Asselbergs FW, De Borst GJ, Aavik E, et al. Microanatomy of the human atherosclerotic plaque by single-cell transcriptomics. *Circ Res.* 2020;127:1437–1455. doi: 10.1161/CIRCRESAHA.120.316770
- Falini B, Flenghi L, Pileri S, Gambacorta M, Bigerna B, Durkop H, Eitelbach F, Thiele J, Pacini R, Cavaliere A, et al. PG-M1: a new monoclonal antibody directed against a fixative-resistant epitope on the macrophage-restricted form of the CD68 molecule. *Am J Pathol.* 1993;142:1359–1372.
- Stary HC, Chandler AB, Dinsmore RE, Fuster V, Glagov S, Insull W Jr, Rosenfeld ME, Schwartz CJ, Wagner WD, Wissler RW. A definition of advanced types of atherosclerotic lesions and a histological classification of atherosclerosis. a report from the Committee on Vascular Lesions of the Council on Arteriosclerosis, American Heart Association. *Circulation.* 1995;92:1355–1374. doi: 10.1161/01.cir.92.5.1355
- Zirngibl RA, Senis Y, Greer PA. Enhanced endotoxin sensitivity in fps/fes-null mice with minimal defects in hematopoietic homeostasis. *Mol Cell Biol.* 2002;22:2472–2486. doi: 10.1128/MCB.22.8.2472-2486.2002
- Liu M, Zhang W, Li X, Han J, Chen Y, Duan Y. Impact of age and sex on the development of atherosclerosis and expression of the related genes in apoE deficient mice. *Biochem Biophys Res Commun.* 2016;469:456–462. doi: 10.1016/j.bbrc.2015.11.064
- Zhang G, Li C, Zhu N, Chen Y, Yu Q, Liu E, Wang R. Sex differences in the formation of atherosclerosis lesion in apoE(-/-) mice and the effect of 17 $\beta$ -estradiol on protein S-nitrosylation. *Biomed Pharmacother.* 2018;99:1014–1021. doi: 10.1016/j.biopha.2018.01.145
- Fairfax BP, Humburg P, Makino S, Naranbhai V, Wong D, Lau E, Jostins L, Plant K, Andrews R, McGee C, et al. Innate immune activity conditions the effect of regulatory variants upon monocyte gene expression. *Science.* 2014;343:1246949. doi: 10.1126/science.1246949
- Zeller T, Wild P, Szymczak S, Rotival M, Schillert A, Castagne R, Maoche S, Germain M, Lackner K, Rossmann H, et al. Genetics and beyond—the transcriptome of human monocytes and disease susceptibility. *PLoS One.* 2010;5:e10693. doi: 10.1371/journal.pone.0010693
- Solomon CU, McVey DG, Andreadi C, et al. Effects of coronary artery disease-associated variants on vascular smooth muscle cells. *Circulation.* 2022;146:917–929. doi: 10.1161/CIRCULATIONAHA.121.058389
- Kheradpour P, Kellis M. Systematic discovery and characterization of regulatory motifs in ENCODE TF binding experiments. *Nucleic Acids Res.* 2014;42:2976–2987. doi: 10.1093/nar/gkt1249
- Nadeau S, Martins GA. Conserved and unique functions of blimp1 in immune cells. *Front Immunol.* 2021;12:805260. doi: 10.3389/fimmu.2021.805260
- Yu J, Angelin-Duclos C, Greenwood J, Liao J, Calame K. Transcriptional repression by blimp-1 (PRDI-BF1) involves recruitment of histone deacetylase. *Mol Cell Biol.* 2000;20:2592–2603. doi: 10.1128/MCB.20.7.2592-2603.2000
- Lord CA, Savitsky D, Sitcheran R, Calame K, Wright JR, Ting JP, Williams KL. Blimp-1/PRDM1 mediates transcriptional suppression of the NLR gene NLRP12/Monarch-1. *J Immunol.* 2009;182:2948–2958. doi: 10.4049/jimmunol.0801692
- Minnich M, Tagoh H, Bonelt P, Axelsson E, Fischer M, Cebolla B, Tarakhovskiy A, Nutt SL, Jaritz M, Busslinger M. Multifunctional role of the transcription factor Blimp-1 in coordinating plasma cell differentiation. *Nat Immunol.* 2016;17:331–343. doi: 10.1038/ni.3349
- Gyory I, Wu J, Fejer G, Seto E, Wright KL. PRDI-BF1 recruits the histone H3 methyltransferase G9a in transcriptional silencing. *Nat Immunol.* 2004;5:299–308. doi: 10.1038/ni1046

34. Liu B, Pjanic M, Wang T, Nguyen T, Gloude-mans M, Rao A, Castano VG, Nurnberg S, Rader DJ, Elwyn S, et al. genetic regulatory mechanisms of smooth muscle cells map to coronary artery disease risk loci. *Am J Hum Genet*. 2018;103:377–388. doi: 10.1016/j.ajhg.2018.08.001
35. Ray-Gallet D, Mao C, Tavitian A, Moreau-Gachelin F. DNA binding specificities of Spi-1/PU.1 and Spi-B transcription factors and identification of a Spi-1/Spi-B binding site in the c-fes/c-fps promoter. *Oncogene*. 1995;11:303–313.
36. Heydemann A, Juang G, Hennessy K, Parmacek MS, Simon MC. The myeloid-cell-specific c-fes promoter is regulated by Sp1, PU.1, and a novel transcription factor. *Mol Cell Biol*. 1996;16:1676–1686. doi: 10.1128/MCB.16.4.1676
37. Heydemann A, Boehmler JH, Simon MC. Expression of two myeloid cell-specific genes requires the novel transcription factor, c-fes expression factor. *J Biol Chem*. 1997;272:29527–29537. doi: 10.1074/jbc.272.47.29527
38. He Y, Borellini F, Koch WH, Huang KX, Glazer RI. Transcriptional regulation of c-Fes in myeloid leukemia cells. *Biochim Biophys Acta*. 1996;1306:179–186. doi: 10.1016/0167-4781(96)00005-x
39. Heydemann A, Warming S, Clendenin C, Sigrist K, Hjorth JP, Simon MC. A minimal c-fes cassette directs myeloid-specific expression in transgenic mice. *Blood*. 2000;96:3040–3048. doi: 10.1182/blood.V96.9.3040
40. Haigh JJ, Ema M, Haigh K, Gertsenstein M, Greer P, Rossant J, Nagy A, Wagner EF. Activated Fps/Fes partially rescues the in vivo developmental potential of Flk1-deficient vascular progenitor cells. *Blood*. 2004;103:912–920. doi: 10.1182/blood-2003-07-2343
41. Sangrar W, Mewburn JD, Vincent SG, Fisher JT, Greer PA. Vascular defects in gain-of-function fps/fes transgenic mice correlate with PDGF- and VEGF-induced activation of mutant Fps/Fes kinase in endothelial cells. *J Thromb Haemost*. 2004;2:820–832. doi: 10.1111/j.1538-7836.2004.00654.x
42. Senis YA, Sangrar W, Zirngibl RA, Craig AW, Lee DH, Greer PA. Fps/Fes and Fer non-receptor protein-tyrosine kinases regulate collagen- and ADP-induced platelet aggregation. *J Thromb Haemost*. 2003;1:1062–1070. doi: 10.1046/j.1538-7836.2003.t01-1-00124.x.
43. Truesdell PF, Zirngibl RA, Francis S, Sangrar W, Greer PA. Fps/fes knock-out mice display a lactation defect and the fps/fes tyrosine kinase is a component of E-cadherin-based adherens junctions in breast epithelial cells during lactation. *Exp Cell Res*. 2009;315:2929–2940. doi: 10.1016/j.yexcr.2009.08.021
44. Mukherji M, Brill LM, Ficarro SB, Hampton GM, Schultz PG. A phosphoproteomic analysis of the ErbB2 receptor tyrosine kinase signaling pathways. *Biochemistry*. 2006;45:15529–15540. doi: 10.1021/bi060971c
45. Li J, Smithgall TE. Fibroblast transformation by Fps/Fes tyrosine kinases requires Ras, Rac, and Cdc42 and induces extracellular signal-regulated and c-Jun N-terminal kinase activation. *J Biol Chem*. 1998;273:13828–13834. doi: 10.1074/jbc.273.22.13828
46. Laurent CE, Smithgall TE. The c-Fes tyrosine kinase cooperates with the breakpoint cluster region protein (Bcr) to induce neurite extension in a Rac- and Cdc42-dependent manner. *Exp Cell Res*. 2004;299:188–198. doi: 10.1016/j.yexcr.2004.05.010
47. Chen Y, Yang Z, Meng M, Zhao Y, Dong N, Yan H, Liu L, Ding M, Peng HB, Shao F. Cullin mediates degradation of RhoA through evolutionarily conserved BTB adaptors to control actin cytoskeleton structure and cell movement. *Mol Cell*. 2009;35:841–855. doi: 10.1016/j.molcel.2009.09.004
48. Siripurapu V, Meth J, Kobayashi N, Hamaguchi M. DBC2 significantly influences cell-cycle, apoptosis, cytoskeleton and membrane-trafficking pathways. *J Mol Biol*. 2005;346:83–89. doi: 10.1016/j.jmb.2004.11.043
49. Kyaw T, Loveland P, Kanellakis P, Cao A, Kallies A, Huang AL, Peter K, Toh BH, Bobik A. Alarmin-activated B cells accelerate murine atherosclerosis after myocardial infarction via plasma cell-immunoglobulin-dependent mechanisms. *Eur Heart J*. 2021;42:938–947. doi: 10.1093/eurheartj/ehaa995